AGU100 ADVANCING EARTH AND SPACE SCIENCE

Geophysical Research Letters

RESEARCH LETTER
10.1029/2018GL079494

Key Points:
- The frequency of the extreme cold/moderate warm events increases in the central equatorial Pacific under recent global warming
- The positive cold tongue mode induces intensification, contraction, and westward shift of Walker circulation and uplift of the thermocline
- The positive cold tongue mode enlarges the sea surface temperature morphology changes of El Niño but covers up those of La Niña

Correspondence to:
C. Zhu,
zhucw@cma.gov.cn

Citation:
Jiang, N., & Zhu, C. (2018). Asymmetric changes of ENSO diversity modulated by the cold tongue mode under recent global warming. *Geophysical Research Letters*, *45*, 12,506–12,513. https://doi.org/10.1029/2018GL079494

Received 6 JUL 2018
Accepted 15 OCT 2018
Accepted article online 17 OCT 2018
Published online 23 NOV 2018

Asymmetric Changes of ENSO Diversity Modulated by the Cold Tongue Mode Under Recent Global Warming

Ning Jiang[1] **and Congwen Zhu**[1]

[1]State Key Laboratory of Severe Weather (LASW) and Institute of Climate System, Chinese Academy of Meteorological Sciences, Beijing, China

Abstract Instead of the La Niña events with no significant change in their surface expressions, the recent increasing frequency of central Pacific El Niño events is suggested to be related to global warming. There is yet no consensus on the impacts of the recent global warming on such asymmetric changes of El Niño-Southern Oscillation (ENSO) events. Here we show the frequency of the extreme cold/moderate warm events both increases in the central equatorial Pacific over the past decades. We attribute the change of ENSO diversity to the positive cold tongue mode under recent global warming, which gives rise to an intensification, contraction, and westward shift of Walker circulation accompanied by an uplift of the thermocline. Our results propose a unified explanation for the changes of ENSO diversity under the recent global warming, which carries important implications for the relationship between global warming and ENSO.

Plain Language Summary El Niño-Southern Oscillation (ENSO) events, characterized by sea surface temperature anomaly patterns in the tropical Pacific, have great global climate impacts by alternating between warm El Niño and cold La Niña phases. At the expense of the conventional El Niño peaking in the eastern Pacific, the recent increasing frequency of El Niño events with warming sea surface temperature anomalies concentrated in the central equatorial Pacific is suggested to be related to global warming, whereas for the La Niña events, there seems to be no significant change in their surface expressions. There is yet no consensus on the impacts of the recent global warming on such asymmetric changes of ENSO events. Our results show the increasing frequency of both the extreme cold and moderate warm events (ENSO diversity) can be ascribed to the positive cold tongue mode under the recent global warming. The positive cold tongue mode gives rise to an intensification, contraction, and westward shift of Walker circulation accompanied by an uplift of the thermocline, which enlarges the sea surface temperature morphology changes of El Niño but covers up the surface expression of La Niña.

1. Introduction

El Niño-Southern Oscillation (ENSO) events, characterized by sea surface temperature (SST) anomaly patterns in the tropical Pacific, have great global climate impacts by alternating between warm El Niño and cold La Niña phases. ENSO events are characterized by warming or cooling SST anomalies in the eastern equatorial Pacific, and a common way to highlight ENSO diversity is to compare SST anomaly patterns at the peak of different ENSO events (Capotondi et al., 2015). Asymmetric changes of ENSO have been reported over the last 30 years. Compared to prior decades, El Niño events have occurred more frequently, with warming SST anomaly peaking nearer to the dateline (usually named as central Pacific [CP] El Niño), with no significant warming of the east Pacific cold tongue region (Capotondi et al., 2015; Lee & McPhaden, 2010). Meanwhile, the La Niña events show subtler changes in their surface spatial patterns (Ashok et al., 2017; Capotondi et al., 2015; Jadhav et al., 2015; Kug & Ham, 2011; Marathe et al., 2015; Ren & Jin, 2011).

These asymmetric changes of ENSO diversity stimulate most research to be devoted to CP El Niño events (Capotondi et al., 2015; Li et al., 2017). Particularly, the CP El Niño is also referred to the dateline El Niño (Larkin & Harrison, 2005), El Niño Modoki (Ashok et al., 2007), or warm pool El Niño (Kug et al., 2009). Several possible related mechanisms have been proposed, such as the extratropical Pacific climate variability (e.g., Yu & Kim, 2011), westerly wind bursts (e.g., Chen et al., 2015; Lopez & Kirtman, 2013), and the tropical Pacific background state associated with global warming (e.g., Yeh et al., 2009). Despite the large debates, the mechanism of CP El Niño is still unclear (Ashok et al., 2007; Capotondi et al., 2015; Ding et al., 2015; Larson & Kirtman, 2013; Li et al., 2017; Yeh et al., 2009; Yu & Kim, 2011; Zhang et al., 2014), not to say the

asymmetric changes of ENSO diversity and the impacts of the recent global warming. Here we examine the issue using various observations and reveal that the positive cold tongue mode (CTM), which is characterized by a cold SST anomaly in the Pacific cold tongue region and a warm SST anomaly in the rest of the tropical Pacific, induces more extreme cold/moderate warm events peaking near the CP, as well as the potential mechanisms with robust evidence.

2. Data and Method

In the present study, the monthly SST from the Hadley Centre Sea Ice and SST data set version 1 (HadISST1) with a 1° × 1° grid (Rayner et al., 2003) is used. The monthly subsurface variables are obtained from the Simple Ocean Data Assimilation product (SODA 2.2.4) with 0.5° × 0.5° horizontal resolution and 40 vertical levels covering the period 1871–2010 (Carton & Giese, 2008). The atmospheric general circulation data sets are taken from the National Centers for Environmental Prediction/National Center for Atmospheric Research (NCEP/NCAR) reanalysis products (Kalnay et al., 1996), including horizontal and vertical velocity and sea level pressure (SLP). These variables are gridded at 2.5° × 2.5° resolution and are available from 1948 to present. All these data sets used in this study describe anomalies: the mean seasonal cycle from 1981 to 2010 has been removed. Noted that our results are not sensitive to the selections of different data sets and different periods of climatology confirmed by many previous studies (Ashok et al., 2007; L'Heureux et al., 2013; Li, Li, et al., 2015; Li et al., 2017; Marathe et al., 2015; Zhang et al., 2010).

Global surface air temperature anomalies are obtained from third Met Office Hadley Centre and Climatic Research Unit Global Land and Sea Surface Temperature Data Set (HadCRUT4.5; Morice et al., 2012).

Due to the asymmetries and variances of ENSO, at least two indices are required to capture the essential feature of ENSO diversity (Cai et al., 2015; Takahashi et al., 2011; Vimont et al., 2014). We apply the empirical orthogonal function (EOF) analysis to decompose the spatiotemporal SST anomaly variability into orthogonal modes in terms of principal EOF patterns and associated principal component (PC) time series from 1950 to 2016 in the equatorial domain (30°S–30°N, 110°E–70°W). To assess the impacts of the recent global warming, we mainly focus on the long-term variability for comparison. The EOF results are robustly supported by various SST data sets and different long-term periods (Ashok et al., 2007; L'Heureux et al., 2013; Li, Li, et al., 2015; Li et al., 2017; Marathe et al., 2015; Zhang et al., 2010). The EOF spatial patterns of SST anomaly (multiplied by the square roots of their respective eigenvalues) and their corresponding normalized PC (NPC) time series are shown in Figure 1. Notice that PCs, which are corresponding to the normalized EOF patterns, represent the denormalized NPCs.

3. Results

3.1. Changes of ENSO Diversity

An ENSO event can be described by an appropriately weighted combination of the three EOF modes. Among them, EOF1 gives the canonical El Niño pattern (Figure 1a; Rasmusson & Carpenter, 1982), and EOF3 (Figure 1e) resembles the Pacific Meridional Mode (Chiang & Vimont, 2004). Here we extract the boreal winter (December-January-February) components of NPCs to describe the ENSO events (Figure 2a). Based on the linear combinations of NPC1 and NPC3, two indices can be used to classify ENSO diversity into two regimes (Takahashi et al., 2011; Vimont et al., 2014): the E-index, defined as $(\mathrm{NPC1}-\mathrm{NPC3})/\sqrt{2}$, corresponds to the extreme warm events (stars in Figure 2a), while the C-index, as $(\mathrm{NPC1}+\mathrm{NPC3})/\sqrt{2}$, is corresponding to the extreme cold/moderate warm events in the central equatorial Pacific.

EOF2 shares some characteristics with EOF1 (Figure 1c), representing an out-of-phase relationship of SST anomaly variability between the Pacific cold tongue region and else in the tropical Pacific, but its existence strongly depends on the linear trends of SST over the tropical Pacific Ocean (L'Heureux et al., 2013). This mode, as a coupled air-sea mode, is named as CTM (Zhang et al., 2010), which becomes the third mode in the recent short period (e.g., Ashok et al., 2007). Its long-term variability and its recent persistent positive phase have been speculated to be a response of ocean dynamical processes to the recent global warming (Li, Li, et al., 2015). The frequent CP El Niño started appearing since the CTM changed to a positive phase in the 1980s (Li et al., 2017), which suggests that the CTM may act as a bridge linking the recent global warming with the change of ENSO diversity.

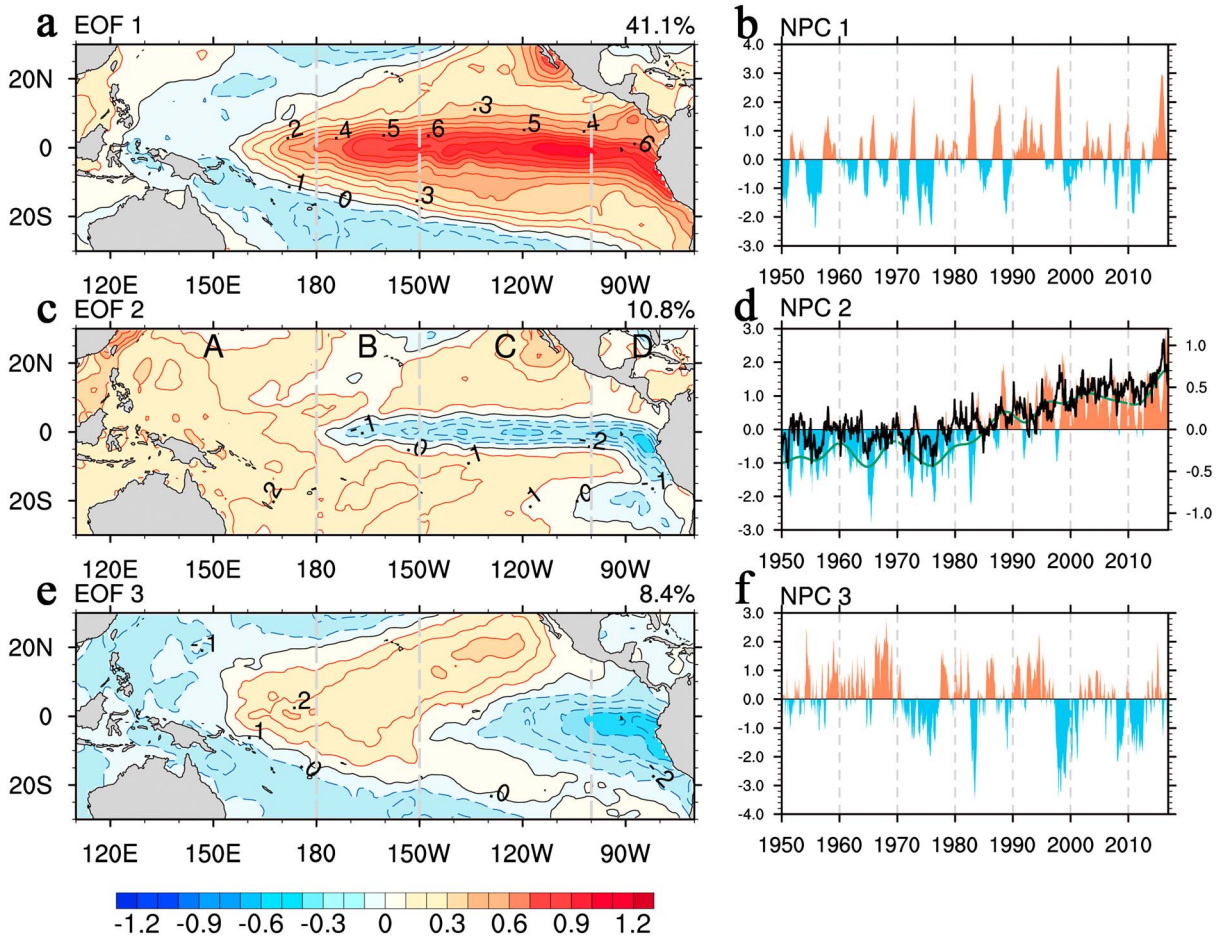

Figure 1. The empirical orthogonal function (EOF) analysis of tropical Pacific sea surface temperature anomaly variability during 1950–2016. (a, c, and e) The three leading EOF modes (unit: K) and (b, d, and f) their corresponding normalized principal components (NPCs; scale on the left axis). The low-frequency component of NPC2 (green line; scale on left axis) and the time series of monthly mean global surface air temperature anomaly (black line; scale on right axis) are plotted in d. The low-frequency component of NPC2 is obtained from a 7-year Lanczos low-pass filter (green line in d).

The CTM acts as a trend mode (Ashok et al., 2007; L'Heureux et al., 2013; Zhang et al., 2010), and we mainly focus on the impacts associated with its trend or its phase transition rather than its high-frequency fluctuations. In order to depict its phase transition clearly, a 7-year Lanczos low-pass filter was applied to remove the high-frequency variability from NPC2. Then the positive (negative) CTM phase can be defined as the filtered NPC2 greater (less) than 0.25 (−0.25) standard deviation (*SD*) amplitude objectively.

Considering the large amplitude of EOF1 in the eastern equatorial region, the EOF2 and EOF3 usually act as two *modulators* determining the interevent differences in SST (e.g., Ashok et al., 2007, 2012; Cai et al., 2015; Capotondi et al., 2015; Li et al., 2017; Takahashi et al., 2011). To detail the change of ENSO diversity related to CTM, first, we compare the ENSO events between the positive and negative phases of CTM in the NPC-related space.

In the positive phase of CTM, the recent ENSO diversity turns close to the regime of extreme cold/moderate warm events peaking in the CP, indicated by the shift of regression line as well as the change of C-index in Figure 2a. The two modes, EOF1 and EOF3, tend to occur in the same phases during the boreal winter (December-January-February). Then the amplitudes of ENSO-related SST anomaly tend to be enhanced and weakened in the central and the eastern Pacific, respectively. These results are also supported by the trend and skewness of the C-index even including the extreme warm events (Takahashi et al., 2011).

Linear contributions of EOF2 and EOF3 can be quantified by comparing the variances of each mode, which can be determined by their corresponding PCs. For instance, in Figure 2a the events with light blue year labels indicate that the amplitude of PC2 is smaller than that of PC3. That is to say, compared to CTM the

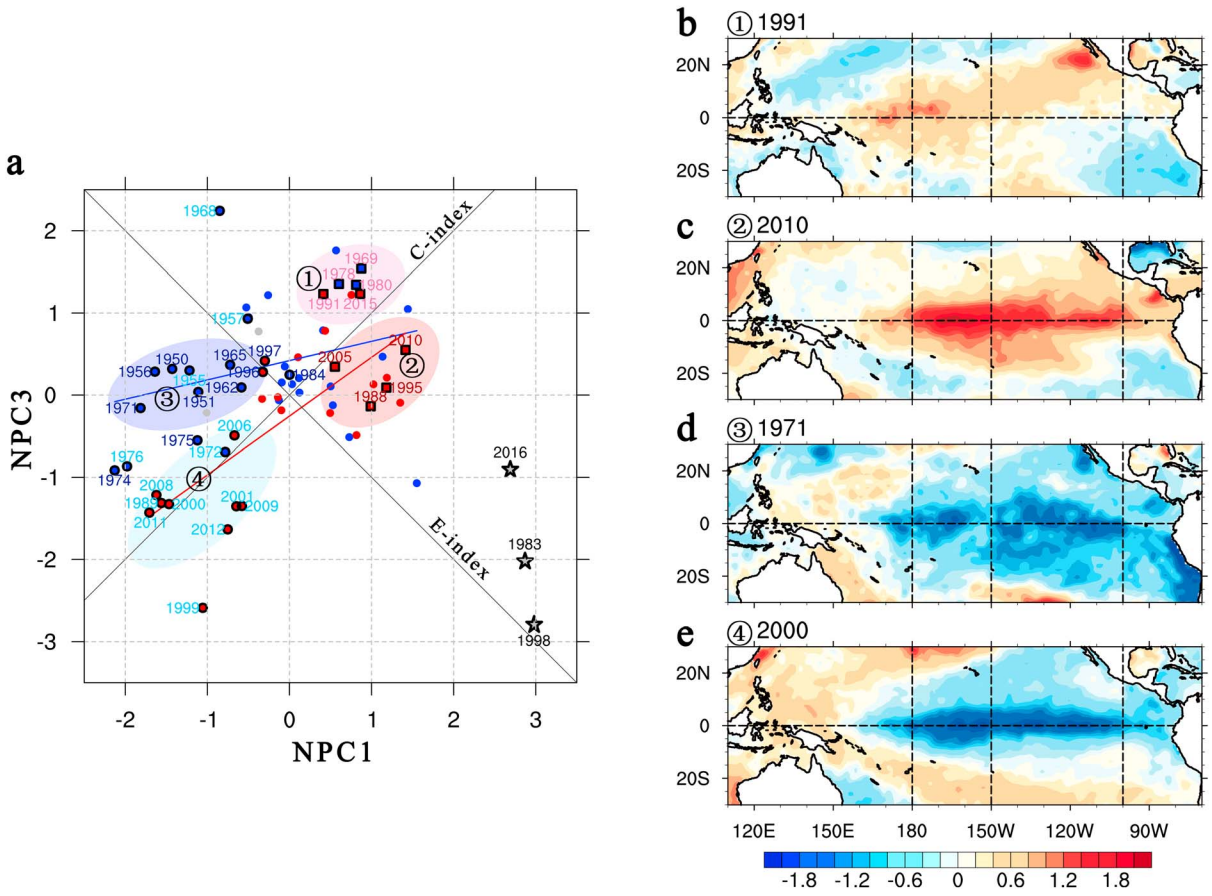

Figure 2. Distribution of boreal winter sea surface temperature (SST) anomaly spatial pattern in the normalized principal component (NPC)-space and SST anomaly spatial patterns of different types of El Niño-Southern Oscillation (ENSO) events. (a) Scatter plot of December–February (DJF) mean NPC1 (*x* axis) and NPC3 (*y* axis). The stars indicate extreme El Niño events defined as NPC1 greater than 2 standard deviation (*SD*) amplitude; the red (blue) dots indicate the events in the positive (negative) phase of the cold tongue mode except the extreme El Niño events, which is defined as the low-frequency component of NPC2 (green line in Figure 1d) greater (less) than 0.25 (−0.25) *SD* amplitude and NPC1 less than 2 *SD* amplitude; the black circles indicate the La Niña events defined as any of DJF mean Niño 3 index, Niño 4 index, and Niño 3.4 index less than −0.5 K. The black boxes indicate the central Pacific El Niño events defined as any of DJF mean Niño 3 index, Niño 4 index, and Niño 3.4 index greater than 0.5 K and DJF mean Niño 4 index greater than Niño 3 index. The dark (light) blue and red year labels indicate the La Niña and the CP El Niño events defined as the amplitude of PC2 greater (less) than that of PC3, respectively. The red (blue) linear regression line of the red (blue) dots indicates the ENSO regime system in positive (negative) phase of the cold tongue mode. The year labels indicate the year of January and February (i.e., 1998 indicates 1997(D)–1998(JF)). (b–e) The spatial patterns of SST anomaly for specific warm and cold events of either type are shown (marker by the corresponding number), with a contour interval of 0.2 K.

negative EOF3 mode plays a more important role in modulating the SST anomaly spatial patterns of the recent extreme cold events. Hence, based on the ENSO phases and the relative contributions of the last two EOF modes, the events mainly are divided into four groups in the NPC-related space in Figure 2a.

In spite of no significant change in surface expression for La Niña events, a clear shift can be identified in the NPC-related space (from group3 to group 4 in Figure 2a), implying the great linear modulation effect of EOF3. Whereas the recent SST changes of El Niño are mainly attributed to linear modulation effect of CTM (group 2), such as the basin warming (Ashok et al., 2012; Figure 2c) and some CP El Niño events (group 2 in Figure 2a). In short, influenced by the positive CTM, frequencies of both moderate El Niño and extreme La Niña events increased, and both of these El Niño and La Niña events are usually accompanied by cold SST anomalies in the tropical eastern Pacific (80–100°W). These frequent cold SST anomalies in the tropical eastern Pacific (80–100°W) enlarge the SST morphology changes of El Niño but cover up those of La Niña. Thus, this makes the ENSO behavior looks asymmetric on the SST anomaly pattern.

3.2. Potential Mechanism

Fedorov and Philander (2000) indicated that the global warming may affect ENSO by altering the background of SST anomaly. The CTM, as a couple air-sea mode, includes several components, such as

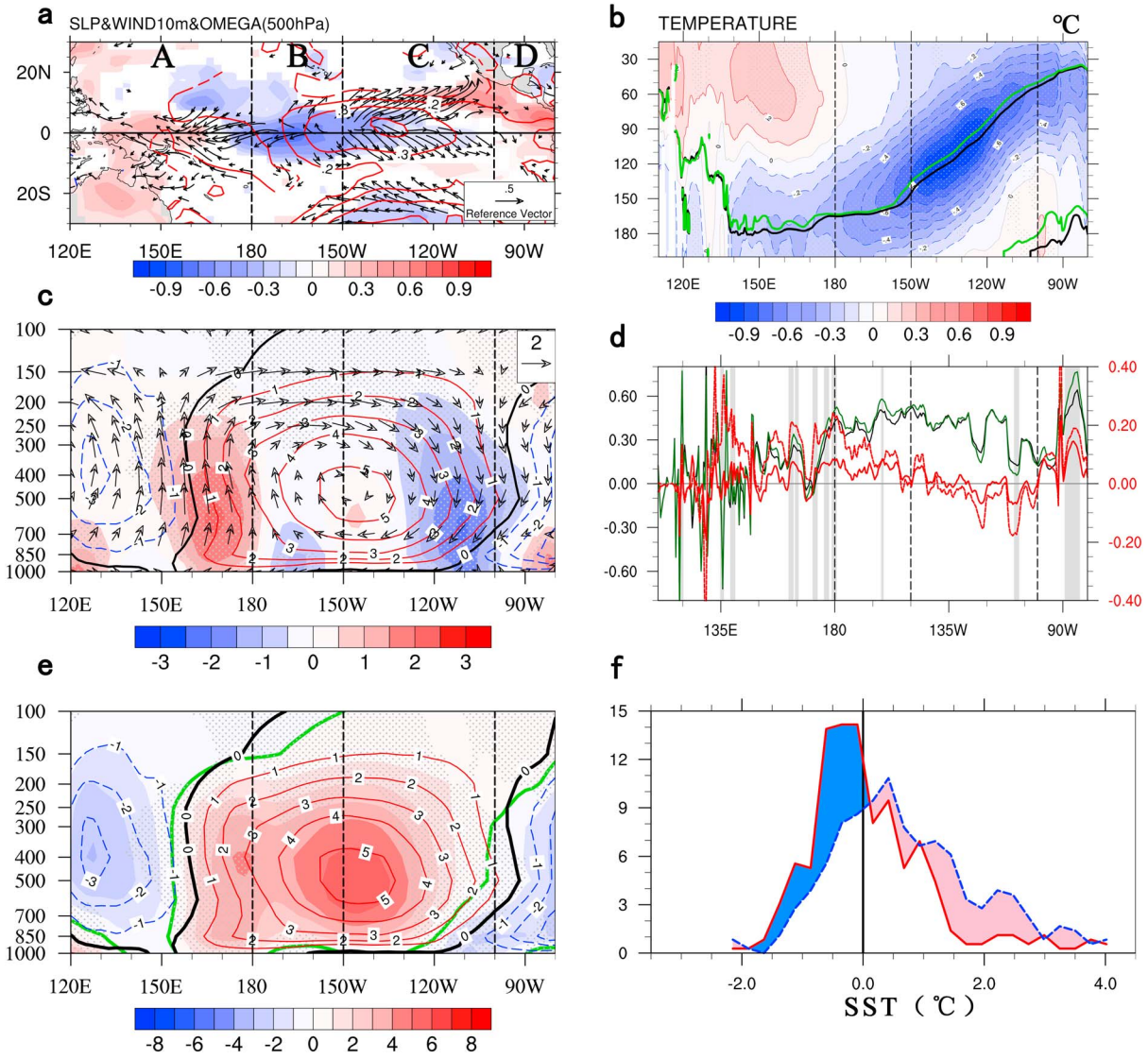

Figure 3. Changes of the atmospheric and oceanic conditions due to the phase switch of cold tongue mode. The atmospheric (oceanic) condition is shown in the left (right) panel. (a) Cold tongue mode (CTM)-regressed sea surface pressure (contour, 0.1-hPa interval), horizontal wind at 10 m (vectors), and 500 hPa vertical wind (shading, omega×-50, positive: upward; Pa/s). (c) The CTM-regressed zonal mass streamfunction (shading; 10^9 kg/s) along the equatorial Pacific (5°S–5°N) and the mean state of zonal mass streamfunction (contours, 10^9 kg/s), pressure velocity (omega× -50; Pa/s), and zonal divergent wind (m/s). (e) Changes of streamfunction (shading, zero line in green) obtained by the sum of CTM-regressed streamfunction (shading in c) and the mean state (contour in c or blue, red, and black contours in e). (b) The CTM-regressed subsurface temperature (5°S–5°N, shading, 0.1 K interval) and the thermocline depth (mean state: black solid line; mean state + cold tongue part: green solid line). The regression values plotted in a and dotted in b, c, and e are statistically significant above the 95% confidence level. d CTM-regressed (scale on right axis) and the mean state (scale on left axis) vertical currents (positive upward, 10^{-5} m/s) averaged over 5°S to 5°N are illustrated by the red solid line and the black solid line, respectively. The green solid line (scale on left axis) indicates the sum of them two (the red solid and black solid lines). The pink dashed line (scale on right axis) is for the regressed vertical current averaged over 2°S to 2°N (statistical significance at the 95% confidence level are marked by the gray-filled bars). (f) The frequency distributions of the SST anomaly averaged from 5°S to 5°N in the east of 100°W (80–100°W marked by "D" in a) of 1950–1979 (blue dashed line) and 1987–2016 (red solid line).

atmospheric and oceanic circulation fields, and may act as a response to the recent global warming (Clement et al., 1996; Li, Li, et al., 2015; Zhang et al., 2010). To reveal the possible impacts of the CTM on the changes of ENSO under recent global warming, we examine the positive phase of CTM and their joint effects with the mean states.

The atmospheric and oceanic conditions associated with CTM are reflected by CTM-regressed components (Li, Li, et al., 2015; Zhang et al., 2010), obtained through linear regression onto the NPC2 monthly time series from 1950 to 2016, and we only focus on regression values with statistical significance at the 95% confidence

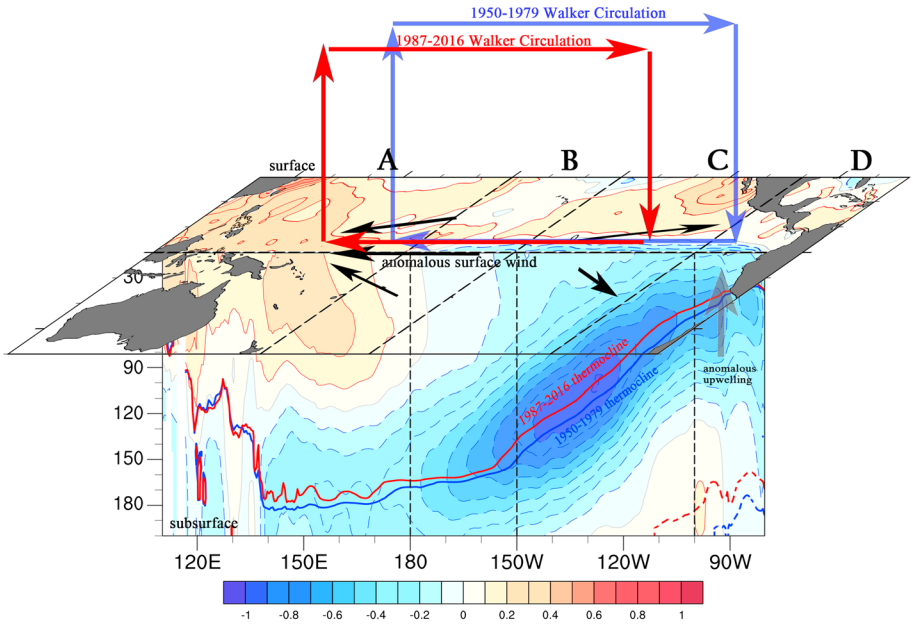

Figure 4. Schematic of the changes of the ocean-atmosphere in the Pacific due to the phase switch of cold tongue mode. Color shading shows sea surface (refer to Figure 1c and Northern Hemisphere only) and subsurface (averaged between 5°S and 5°N; refer to Figure 3b) temperature anomaly of the cold tongue mode. The red (blue) arrows indicate the Walker circulation, and the red (blue) solid line shows thermocline in the subsurface respectively during 1987–2016 (1950–1979). The anomalous atmospheric circulations near the sea surface are indicated by black thin arrows (refer to Figure 3a), and the anomalous subsurface upwelling in the eastern tropical Pacific (refer to Figure 3d) is illustrated by a thick gray arrow.

level. The NPC2 reflects the intensity and phase of all the regressed components of CTM. For instance, when the NPC2 value is 1, the CTM components show a positive phase with 1 *SD* amplitude. Similarly, the NPC2 equals to −1, the CTM components are in the negative phase with −1 *SD* amplitude. In Figure 3, to assess the joint effects of the positive CTM components and the mean state (annual mean), we simply combine the regressed CTM components (NPC2 is set to 1) with the mean state. Noted the average NPC2 over 1987 to 2016 (1950 to 1979) is 0.87 (−0.76), representing the differences of phase and intensity of CTM in the two periods. These two periods are used to compare the changes in the air-sea system due to the phase switch of CTM (Figure 4).

The positive CTM phase induces an anomalous zonal gradient of SLP in the west of the dateline and meridional gradients of SLP in the east of 150°W (Figure 3a). The anomalous SLP gradient strengthens the trade winds in the west of the dateline, whereas, considering the effect of Coriolis force, it reduces the trade winds in the east of 150°W (Figure 3a), which brings strong divergence anomalies over the eastern equatorial Pacific (Li, Li, et al., 2015; Zhang et al., 2010). The anomalous SLP and trade winds associated with CTM also produce two anomalous vertical circular circulations (Figure 3c), which causes an intensification, contraction, and westward shift of the Walker circulation (Figure 3e). The changes in trade winds and Walker circulation under the positive CTM phase and their joint effects with the mean states seem to induce a westward shift of the air-sea action center of ENSO, accounting for the frequent ENSO events peaking in the CP. And the strengthened Walker circulation can result in the asymmetric intensity of ENSO events, as more extreme La Niña and moderate El Niño events (Li et al., 2017; Takahashi et al., 2011).

In the ocean, corresponding to the positive CTM, the cold subsurface sea temperature anomalies under the eastern Pacific shrink to the bottom of western Pacific with a warm center above, which induces an uplift of the thermocline (Figure 3b; Li, Li, et al., 2015; Solomon & Newman, 2012). Notice that the subsurface anomalous cooling center with the biggest uplift of thermocline between 120 and 150°W causes a greater tilt of thermocline in the western Pacific and flattens the shallower thermocline in the eastern Pacific (Figure 3b). The changes of the thermocline tilt are consistent with the changes of the trade winds and the Walker circulation. And the shallower thermocline in the west of 100°W with the westward Walker circulation is conducive to the development of the air-sea interaction in the CP.

On the other hand, the CTM-associated anomalous upwelling in the east of 100°W (Figure 3d), accompanied by the mean upwelling and a shallower thermocline in the eastern Pacific (80–100°W; Figure 3b), makes the SST anomalies easier to get cold mainly through the vertical advection. And this anomalous upwelling may be due to the strengthened divergence of wind stress (Figure 3a; Li, Li, et al., 2015). These changes in the eastern Pacific explain the frequent cold SST anomalies in the tropical eastern Pacific (east of 100°W and marked by "D" in Figure 3) since the 1980s. The frequent cold SST anomalies in the eastern tropical Pacific (5°S–5°N, 80–100°W) can be identified by comparing the frequency distributions of the tropical eastern Pacific SST anomalies between 1950–1979 (the first 30 years of negative CTM) and 1987–2016 (the last 30 years of positive CTM; Figure 3f). The differences of SST anomalies in the eastern tropical Pacific (5°S–5°N, 80–100°W) between these two periods are significant at 5% level through Student's *t* test.

4. Summary and Discussion

To comprehensive depict the CTM-associated changes and the impacts on the changes of ENSO diversity, a schematic diagram is illustrated by a comparison between 1950–1979 and 1987–2016 (Figure 4). In summary, the CTM, as a couple air-sea mode, may act as a bridge linking ENSO with the recent global warming and is responsible for the intensification, contraction, and westward shift of Walker circulation with an uplift of the thermocline, as well as the anomalous upwelling in the eastern tropical Pacific. These CTM-associated changes can explain the recent changes of ENSO diversity, including surface expressions and intensities.

Large discrepancies remain among the various estimates of long-term changes in the tropical Pacific under global warming (e.g., Collins et al., 2010; Vecchi et al., 2008), but in recent decades the La Niña-like SST anomalies with a strengthened walker circulation seems robust (Ma & Zhou, 2016). Particular, the ocean dynamical processes are predominantly responsible for the long-term trend of the CTM in the tropical Pacific (Cane et al., 1997; Clement et al., 1996; Li, Li, et al., 2015; Seager & Murtugudde, 1997; Sun & Liu, 1996; Zhang et al., 2010), where vigorous upwelling of cold water in the eastern equatorial region causes weaker warming in the eastern Pacific than in the western Pacific. Meanwhile, the La Niña-like pattern is also suggested to be modulated by the Atlantic warming under the recent global warming (Li, Xie, et al., 2015; McGregor et al., 2014). The Atlantic warming is likely coming from radiative forcing and Atlantic Multi-decadal Oscillation (Li et al., 2016). The former may be caused by the increase of greenhouse gas (Kucharski et al., 2011), but the latter is possibly resulted from the Atlantic meridional overturning circulation (AMOC) as internal variability.

Besides, the relationship between ENSO and greenhouse warming has been discussed (e.g., Cai et al., 2015; Yeh et al., 2009). However, these results are based on the climate projection from model outputs, and the projected slow-down Walker circulation is opposite to the observation. Our results may provide an important implication for understanding the recent change of ENSO diversity, as well as the climate projection under future climate change.

Acknowledgments
The author acknowledges the anonymous reviewers and Jeremy Cheuk-Hin Leung for their helpful comments and suggestions. This study is jointly supported by the Special Fund for Public Welfare Industry from the Ministry of Finance (MOF) (GYHY20140609), the China NSF (41475057 and 41830969), and the Basic Scientific Research and Operation Foundation of CAMS (2018Z006 and 2018Y003). The HadISST1 and HadCRUT4 data sets were obtained from the Met Office Hadley Centre and can be downloaded from http://www.metoffice.gov.uk/hadobs/hadisst/data/download.html and http://www.cru.uea.ac.uk/cru/data/temperature/, respectively. The SODA data set was obtained from the National Center for Atmospheric Research (NCAR) and can be downloaded from http://dsrs.atmos.umd.edu/DATA/soda_2.2.4/. NCEP Reanalysis data provided by the NOAA/OAR/ESRL PSD, Boulder, Colorado, USA, from their Web site at https://www.esrl.noaa.gov/psd/.

References

Ashok, K., Behera, S. K., Rao, S. A., Weng, H., & Yamagata, T. (2007). El Niño Modoki and its possible teleconnection. *Journal of Geophysical Research*, *112*, C11007. https://doi.org/10.1029/2006JC003798

Ashok, K., Sabin, T. P., Swapna, P., & Murtugudde, R. G. (2012). Is a global warming signature emerging in the tropical Pacific? *Geophysical Research Letters*, *39*, L02701. https://doi.org/10.1029/2011GL050232

Ashok, K., Shamal, M., Sahai, A. K., & Swapna, P. (2017). Nonlinearities in the evolutional distinctions between El Niño and La Niña types. *Journal of Geophysical Research: Oceans*, *122*, 9649–9662. https://doi.org/10.1002/2017JC013129

Cai, W., Santoso, A., Wang, G., Yeh, S.-W., An, S.-I., Cobb, K. M., et al. (2015). ENSO and greenhouse warming. *Nature Climate Change*, *5*(9), 849–859. https://doi.org/10.1038/nclimate2743

Cane, M. A., Clement, A. C., Kaplan, A., Kushnir, Y., Pozdnyakov, D., Seager, R., et al. (1997). Twentieth-century sea surface temperature trends. *Science*, *275*(5302), 957–960. https://doi.org/10.1126/science.275.5302.957

Capotondi, A., Wittenberg, A. T., Newman, M., Di Lorenzo, E., Yu, J.-Y., Braconnot, P., et al. (2015). Understanding ENSO diversity. *Bulletin of the American Meteorological Society*, *96*(6), 921–938. https://doi.org/10.1175/BAMS-D-13-00117.1

Carton, J. A., & Giese, B. S. (2008). A reanalysis of ocean climate using Simple Ocean Data Assimilation (SODA). *Monthly Weather Review*, *136*(8), 2999–3017. https://doi.org/10.1175/2007MWR1978.1

Chen, D., Lian, T., Fu, C., Cane, M. A., Tang, Y., & Murtugudde, R. (2015). Strong influence of westerly wind bursts on El Niño diversity. *Nature Publishing Group*, *8*(5), 339–345. https://doi.org/10.1038/ngeo2399

Chiang, J. C. H., & Vimont, D. J. (2004). Analogous Pacific and Atlantic meridional modes of tropical atmosphere-ocean variability. *Journal of Climate*, *17*(21), 4143–4158. https://doi.org/10.1175/JCLI4953.1

Clement, A. C., Seager, R., Cane, M. A., & Zebiak, S. E. (1996). An ocean dynamical thermostat. *Journal of Climate*, *9*(9), 2190–2196. https://doi.org/10.1175/1520-0442(1996)009<2190:AODT>2.0.CO;2

Collins, M., An, S.-I., Cai, W., Ganachaud, A., Guilyardi, E., Jin, F.-F., et al. (2010). The impact of global warming on the tropical Pacific Ocean and El Niño. *Nature Geoscience*, *3*(6), 391–397. https://doi.org/10.1038/ngeo868

Ding, R., Li, J., Tseng, Y., Sun, C., & Guo, Y. (2015). The Victoria mode in the North Pacific linking extratropical sea level pressure variations to ENSO. *Journal of Geophysical Research: Atmospheres*, *120*, 27–45. https://doi.org/10.1002/2014JD022221

Fedorov, A. V., & Philander, S. G. (2000). Is El Niño changing? *Science*, *288*(5473), 1997–2002. https://doi.org/10.1126/science.288.5473.1997

Jadhav, J., Panickal, S., Marathe, S., & Ashok, K. (2015). On the possible cause of distinct El Niño types in the recent decades. *Scientific Reports*, *5*(1), 17009. https://doi.org/10.1038/srep17009

Kalnay, E., Kanamitsu, M., Kistler, R., Collins, W., Deaven, D., Gandin, L., et al. (1996). The NCEP/NCAR 40-Year Reanalysis Project. *Bulletin of the American Meteorological Society*, *77*(3), 437–471. https://doi.org/10.1175/1520-0477(1996)077<0437:TNYRP>2.0.CO;2

Kucharski, F., Kang, I.-S., Farneti, R., & Feudale, L. (2011). Tropical Pacific response to 20th century Atlantic warming. *Geophysical Research Letters*, *38*, L03702. https://doi.org/10.1029/2010GL046248

Kug, J.-S., & Ham, Y.-G. (2011). Are there two types of La Niña? *Geophysical Research Letters*, *38*, L16704. https://doi.org/10.1029/2011GL048237

Kug, J.-S., Jin, F.-F., & An, S.-I. (2009). Two types of El Niño events: Cold tongue El Niño and warm pool El Niño. *Journal of Climate*, *22*(6), 1499–1515. https://doi.org/10.1175/2008JCLI2624.1

Larkin, N. K., & Harrison, D. E. (2005). Global seasonal temperature and precipitation anomalies during El Niño autumn and winter. *Geophysical Research Letters*, *32*, L16705. https://doi.org/10.1029/2005GL022860

Larson, S., & Kirtman, B. (2013). The Pacific meridional mode as a trigger for ENSO in a high-resolution coupled model. *Geophysical Research Letters*, *40*, 3189–3194. https://doi.org/10.1002/grl.50571

Lee, T., & McPhaden, M. J. (2010). Increasing intensity of El Niño in the central-equatorial Pacific. *Geophysical Research Letters*, *37*, L14603. https://doi.org/10.1029/2010GL044007

L'Heureux, M. L., Collins, D. C., & Hu, Z.-Z. (2013). Linear trends in sea surface temperature of the tropical Pacific Ocean and implications for the El Niño-Southern Oscillation. *Climate Dynamics*, *40*(5–6), 1223–1236. https://doi.org/10.1007/s00382-012-1331-2

Li, X., Xie, S.-P., Gille, S. T., & Yoo, C. (2015). Atlantic-induced pan-tropical climate change over the past three decades. *Nature Climate Change*, *6*(3), 275–279. https://doi.org/10.1038/nclimate2840

Li, X., Xie, S.-P., Gille, S. T., & Yoo, C. (2016). Atlantic-induced pan-tropical climate change over the past three decades. *Nature Climate Change*, *6*(3), 275–279. https://doi.org/10.1038/nclimate2840

Li, Y., Li, J., Zhang, W., Chen, Q., Feng, J., Zheng, F., et al. (2017). Impacts of the Tropical Pacific Cold Tongue Mode on ENSO Diversity under Global Warming. *Journal of Geophysical Research: Oceans*, *122*, 8524–8542. https://doi.org/10.1002/2017JC013052

Li, Y., Li, J., Zhang, W., Zhao, X., Xie, F., & Zheng, F. (2015). Ocean dynamical processes associated with the tropical Pacific cold tongue mode. *Journal of Geophysical Research: Oceans*, *120*, 6419–6435. https://doi.org/10.1002/2015JC010814

Lopez, H., & Kirtman, B. P. (2013). Westerly wind bursts and the diversity of ENSO in CCSM3 and CCSM4. *Geophysical Research Letters*, *40*, 4722–4727. https://doi.org/10.1002/grl.50913

Ma, S., & Zhou, T. (2016). Robust strengthening and westward shift of the tropical Pacific Walker circulation during 1979-2012: A comparison of 7 sets of reanalysis data and 26 CMIP5 models. *Journal of Climate*, *29*(9), 3097–3118. https://doi.org/10.1175/JCLI-D-15-0398.1

Marathe, S., Ashok, K., & Sabin, P. S. T. P. (2015). Revisiting El Niño Modokis. *Climate Dynamics*, 3527–3545. https://doi.org/10.1007/s00382-015-2555-8

McGregor, S., Timmermann, A., Stuecker, M. F., England, M. H., Merrifield, M., Jin, F. F., et al. (2014). Recent walker circulation strengthening and pacific cooling amplified by Atlantic warming. *Nature Climate Change*, *4*(10), 888–892. https://doi.org/10.1038/nclimate2330

Morice, C. P., Kennedy, J. J., Rayner, N. A., & Jones, P. D. (2012). Quantifying uncertainties in global and regional temperature change using an ensemble of observational estimates: The HadCRUT4 data set. *Journal of Geophysical Research*, *117*, D08101. https://doi.org/10.1029/2011JD017187

Rasmusson, E. M., & Carpenter, T. H. (1982). Variations in tropical sea surface temperature and surface wind fields associated with the southern oscillation/El Niño. *Monthly Weather Review*, *110*(5), 354–384. https://doi.org/10.1175/1520-0493(1982)110<0354:VITSST>2.0.CO;2

Rayner, N. A., Parker, D. E., Horton, E. B., Folland, C. K., Alexander, L. V., & Rowell, D. P. (2003). Global analyses of sea surface temperature, sea ice, and night marine air temperature since the late nineteenth century. *Journal of Geophysical Research*, *108*(D14), 4407. https://doi.org/10.1029/2002JD002670

Ren, H. L., & Jin, F. F. (2011). Niño indices for two types of ENSO. *Geophysical Research Letters*, *38*, L04704. https://doi.org/10.1029/2010GL046031

Seager, R., & Murtugudde, R. (1997). Ocean dynamics, thermocline adjustment, and regulation of tropical SST. *Journal of Climate*, *10*(3), 521–534. https://doi.org/10.1175/1520-0442(1997)010<0521:ODTAAR>2.0.CO;2

Solomon, A., & Newman, M. (2012). Reconciling disparate twentieth-century Indo-Pacific ocean temperature trends in the instrumental record. *Nature Climate Change*, *2*(9), 691–699. https://doi.org/10.1038/nclimate1591

Sun, D.-Z., & Liu, Z. (1996). Dynamic ocean-atmosphere coupling: A thermostat for the tropics. *Science*, *272*(5265), 1148–1150. https://doi.org/10.1126/science.272.5265.1148

Takahashi, K., Montecinos, A., Goubanova, K., & Dewitte, B. (2011). ENSO regimes: Reinterpreting the canonical and Modoki El Niño. *Geophysical Research Letters*, *38*, L10707. https://doi.org/10.1029/2011GL047364

Vecchi, G. A., Clement, A., & Soden, B. J. (2008). Examining the tropical Pacific's response to global warming. *Eos, Transactions American Geophysical Union*, *89*(9), 81–83. https://doi.org/10.1029/2008EO090002

Vimont, D. J., Alexander, M. A., & Newman, M. (2014). Optimal growth of central and East Pacific ENSO events. *Geophysical Research Letters*, *41*, 4027–4034. https://doi.org/10.1002/2014GL059997

Yeh, S., Kug, J., Dewitte, B., Kwon, M., Kirtman, B. P., & Jin, F. (2009). El Niño in a changing climate. *Nature*, *461*(7263), 511–514. https://doi.org/10.1038/nature08316

Yu, J. Y., & Kim, S. T. (2011). Relationships between extratropical sea level pressure variations and the central Pacific and eastern Pacific types of ENSO. *Journal of Climate*, *24*(3), 708–720. https://doi.org/10.1175/2010JCLI3688.1

Zhang, H., Clement, A., & Nezio, P. D. (2014). The south pacific meridional mode: A mechanism for ENSO-like variability. *Journal of Climate*, *27*(2), 769–783. https://doi.org/10.1175/JCLI-D-13-00082.1

Zhang, W., Li, J., & Zhao, X. (2010). Sea surface temperature cooling mode in the Pacific cold tongue. *Journal of Geophysical Research*, *115*, C12042. https://doi.org/10.1029/2010JC006501